INFECTION AND IMMUNITY, Jan. 2009, p. 32–44 Vol. 77, No. 1
0019-9567/09/$08.00+0 doi:10.1128/IAI.00772-08

Mode of Expression and Functional Characterization of FCT-3 Pilus Region-Encoded Proteins in *Streptococcus pyogenes* Serotype M49▽†

Masanobu Nakata,[1,5] Thomas Köller,[1] Karin Moritz,[1] Deborah Ribardo,[2] Ludwig Jonas,[3] Kevin S. McIver,[2,4] Tomoko Sumitomo,[5] Yutaka Terao,[5] Shigetada Kawabata,[5] Andreas Podbielski,[1] and Bernd Kreikemeyer[1]*

Institute of Medical Microbiology, Virology and Hygiene, Schillingallee 70, 18055 Rostock, Germany[1]; UT Southwestern Medical Center, Department of Microbiology, 5323 Harry Hines Blvd., Dallas, Texas[2]; Electron Microscopy Centre, Department of Pathology, Medical Faculty, Strempelstrasse 14, 18055 Rostock, Germany[3]; Department of Cell Biology and Molecular Genetics, University of Maryland, Biosciences Research Bldg. (413), College Park, Maryland[4]; and Department of Oral and Molecular Microbiology, Osaka University Graduate School of Dentistry, 1-8 Yamadaoka, Suita-Osaka 565-0871, Japan[5]

Received 19 June 2008/Returned for modification 24 September 2008/Accepted 6 October 2008

The human pathogen *Streptococcus pyogenes* (group A streptococcus [GAS]) pilus components, suggested to play a role in pathogenesis, are encoded in the variable FCT (fibronectin- and collagen-binding T-antigen) region. We investigated the functions of sortase A (SrtA), sortase C2 (SrtC2), and the FctA protein of the most prevalent type 3 FCT region from a serotype M49 strain. Although it is considered a housekeeping sortase, SrtA's activity is involved in pilus formation in addition to its essentiality for GAS extracellular matrix protein binding, host cell adherence/internalization, survival in human blood, and biofilm formation. SrtC2 activity is crucial for pilus formation but dispensable for the other phenotypes tested in vitro. FctA is the major pilus backbone protein, simultaneously acting as the M49 T antigen, and requires SrtC2 and LepA, a signal peptidase I homologue, for monomeric surface expression and polymerization, respectively. Collagen-binding protein Cpa expression supports pilus formation at the pilus base. Immunofluorescence microscopy and fluorescence-activated cell sorting analysis revealed several unexpected expression patterns, as follows: (i) the monomeric pilus protein FctA was found exclusively at the old poles of GAS cells, (ii) FctA protein expression increased with lower temperatures, and (iii) FctA protein expression was restricted to 20 to 50% of a given GAS M49 population, suggesting regulation by a bistability mode. Notably, disruption of pilus assembly by sortase deletion rendered GAS serotype M49 significantly more aggressive in a dermonecrotic mouse infection model, indicating that sortase activity and, consequently, pilus expression allow a subpopulation of this GAS serotype to be less aggressive. Thus, pilus expression may not be a virulence attribute of GAS per se.

Streptococcus pyogenes (group A streptococcus [GAS]) is a bacterial pathogen that is perfectly adapted to colonization, infection, and persistence in its human host (8, 10, 14, 22). Many of the associated virulence factors expressed by this bacterium are encoded in discrete regions of the GAS genome (28). Two of these pathogenicity regions (Mga and FCT [see below]) each comprise genes for secreted and surface-exposed virulence factors and at least one stand-alone transcriptional regulator. These genes have been shown to act together in a growth phase-dependent regulatory network to coordinate GAS host cell adherence, internalization, and intracellular persistence (summarized in references 28 and 29).

The FCT region (*f*ibronectin- and *c*ollagen-binding *T*-antigen region) (6) is present in all GAS genomes specifically tested (26). The FCT region always contains a RALP transcriptional regulator whose type correlates with the type of *emm* pathogenicity region and the preferred infection site of the GAS strain, i.e., the throat or the skin. Since a similar association was also shown for the fibronectin- and collagen-binding proteins encoded by this region, the FCT region gene products could contribute to tissue-specific GAS infection (26, 46).

As schematically depicted in Fig. 1, the FCT region is characterized by (i) a fixed gene order but flexible size and architecture; (ii) a variable composition of monocistronically transcribed genes, encoding at least one or two fibronectin-binding proteins (21, 32, 53, 56); (iii) a *cpa* gene encoding a collagen-binding protein as part of a five-gene operon in selected serotype strains (31); (iv) genes for one or two stand-alone transcriptional regulators (RALP family proteins [19] or MsmR [43]), one of which is either the Nra or the RofA version of a RALP regulator (19, 41, 49); (v) a gene for the GAS T antigen, which is traditionally used in parallel with the M and *emm* typing scheme to differentiate GAS serotypes (6, 36); and finally, (vi) several other genes, encoding, e.g., an alternative sortase, one putative signal peptidase, and two additional surface proteins of GAS, for all of which the precise biological function is only beginning to be defined.

Most recently, the alternative sortase and at least two or three of the additionally encoded surface proteins of the FCT region have been described to be involved in pilus-like structure formation on the surface of GAS (42). Moreover, regions with high homology to the GAS FCT region have also been found in the group B streptococcus (GBS; *Streptococcus aga-*

* Corresponding author. Mailing address: Department of Medical Microbiolology and Hospital Hygiene, University Hospital, Schillingallee 70, D-18057 Rostock, Germany. Phone: 49-381-494-5912. Fax: 49-81-494-5902. E-mail: bernd.kreikemeyer@med.uni-rostock.de.

† Supplemental material for this article may be found at http://iai.asm.org/.

▽ Published ahead of print on 13 October 2008.

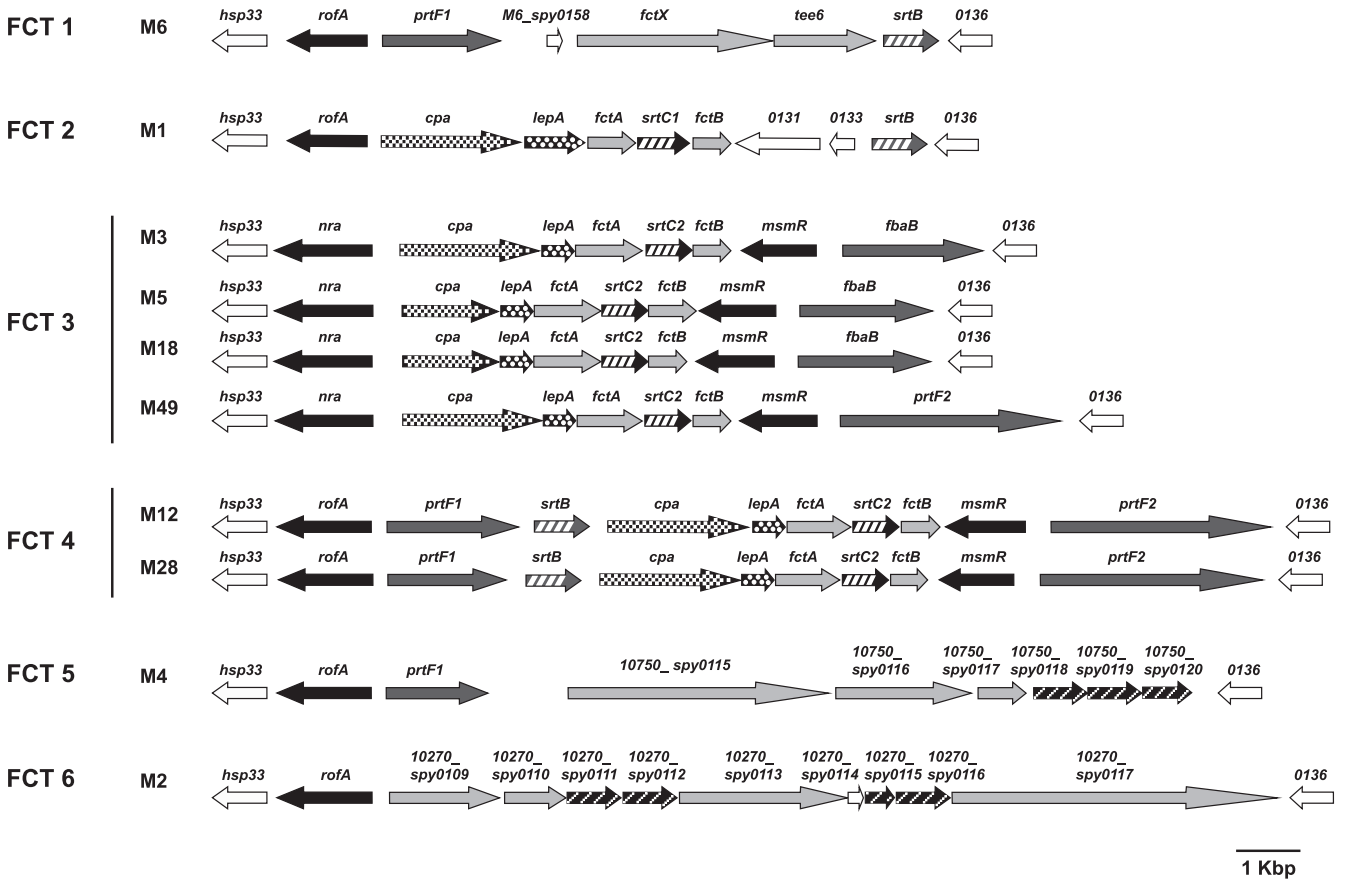

FIG. 1. Gene organization of FCT regions. Genetic heterogeneity of FCT regions from 10 different M serotypes is shown according to publically available sequences. Black arrows, transcriptional regulator genes, including *rofA*, *nra*, and *msmR*; dark gray arrows, fibronectin-binding protein genes, including *prtF1*, *prtF2*, and *fbaB*; light gray arrows, previously reported or inferred surface-expressed protein genes with unknown functions, including *fctA* and *fctB*; pavement-like arrows, collagen-binding protein gene; dark and light gray hatched arrows, sortase genes, including *srtC1*, *srtC2*, *srtB*, and putative genes encoding sortase; white-dotted black arrows, *lepA*; and white arrows, other open reading frames. The spy gene numbers were assigned according to the corresponding genes in the M1 genome sequence. Gene designations are presented above each arrow. *, an internal stop codon is present (codon 218 in *nra* [M18] and codon 102 in *srtB* [M12]). The FCT types are shown according to the work of Kratovac et al. (26). The GenBank accession numbers and strains for each serotype are as follows: M1, NC_002737 and SF370; M2, NC_008022 and MGAS10270; M3, NC_004606 and SSI-1; M4, NC_008024 and MGAS10750; M5, NC_009332 and Manfredo; M6, NC_006086 and MGAS10394; M12, AF447492 and A735; M18, NC_003485 and MGAS8232; and M28, NC_007296 and MGAS6180. The genetic map from a serotype M49 strain is shown based on the genome sequence of strain 591 (7) (GenBank accession no. NZ_AAFV01000006).

lactiae), *Streptococcus pneumoniae*, and *Enterococcus faecalis* (15, 34, 44, 51, 52, 55). In several studies, pili have been shown to be important for streptococcal virulence. GBS pili are involved in bacterial adherence to surfaces of endothelial cells (15, 39), pneumococcal pili influence cell interactions and inflammatory responses (5), and *E. faecalis* pili have a role in biofilm formation and endocarditis (44).

In contrast, for GAS, single pilus components have recently been shown to be important in adhesion to keratinocytes (1), to play a role in a humanized skin infection model, in dependence on the bacterial growth phase (36), and to contribute to bacterial aggregation via FctA-scavenger receptor gp340 interaction (17). However, the assembled pilus is not required for skin virulence per se (36). Additionally, pili of the GAS serotype M1 strain (FCT-2 type) were shown to be important for cell aggregate formation in liquid cultures and microcolony formation on human cells (40).

Pilus proteins could be promising antigens for vaccine development. For pneumococci, GBS, and GAS, it has been shown that a combination of up to four pilus proteins elicits antibodies that are capable of inducing complement-dependent opsonophagocytic killing and conferring protective immunity (18, 38, 42, 55). Finally, GBS pilus components expressed on the surface of *Lactococcus lactis* could be used as a broad-coverage vaccine (9).

The assembly of pili has been studied down to the molecular details for some gram-positive species (55). Restricted data exist on the presence and assembly of pili in GAS. Notably, the structure of the major GAS pilus subunit was recently solved at 2.2-Å resolution (24). The GAS serotype M6 FCT region sortase (SrtB) has been shown to couple the GAS T antigen to the bacterial envelope (4). Another alternative and specialized FCT region-localized sortase version, SrtC2, is responsible for anchoring proteins containing a QVPTG motif to the bacterial cell wall of serotype M3 GAS strains (3).

Like those for the individual alternative sortases, the gene

encoding the putative signal peptidase LepA is apparently only present in selected GAS serotype strains (Fig. 1) (26). For the serotype M3 GAS strains, the signal peptidase SipA was studied and suggested to perform chaperon-like functions (59). However, nothing is known about the role of the putative signal peptidase I (LepA) in virulence expression and modification of other serotype strains and, particularly, in pilus formation of serotype M49 strains. Moreover, it is unclear if all GAS strains express pilus structures in vitro and in vivo even when they harbor an FCT region and, specifically, signal peptidase and sortase genes.

To support the idea of serotype-specific pilus production and to elucidate more details of the LepA and sortase functions, we performed the present study. We used mutational analysis, microscopic techniques, and an animal infection model to study the functions of the GAS serotype M49 FCT-3 region genes as representative of the most frequently occurring FCT region genotype (FCT-3) (26) (Fig. 1).

With our results, we document the crucial role of LepA in pilus assembly. Furthermore, we demonstrate uneven pilus surface expression, mainly at the old poles of GAS cells, and thereby find indications for a bistability expression mode. Finally, we extend data on the FCT-3 region sortase by documenting its virulence-modulating function in a mouse skin infection model.

MATERIALS AND METHODS

Bacterial strains and culture conditions. The GAS serotype M49 strain 591 was obtained from R. Lütticken (Aachen, Germany). The *Escherichia coli* strain DH5α (Gibco-BRL) was used as a host for plasmids pSF151, pFW12, and pAT18 (48, 54, 57). *E. coli* XL10-Gold (Stratagene) served as a host for plasmid pQE30 (Qiagen). All *E. coli* strains were cultured in Luria-Bertani (LB) medium at 37°C with agitation. The GAS wild-type (WT) strain and isogenic derivatives were cultured without agitation in Todd-Hewitt broth (Invitrogen) supplemented with 0.2% yeast extract (THY medium; Invitrogen) at 37°C or 30°C under a 5% CO_2–20% O_2 atmosphere, unless otherwise specified. For selection and maintenance of mutants, antibiotics were added to the media at the following concentrations: ampicillin, 100 μg ml^{-1} for *E. coli*; kanamycin, 50 μg ml^{-1} for *E. coli* and 300 μg ml^{-1} for GAS; spectinomycin, 100 μg ml^{-1} for *E. coli* and 60 μg ml^{-1} for GAS; and erythromycin, 300 μg ml^{-1} for *E. coli* and 5 μg ml^{-1} for GAS.

DNA techniques. Purification of chromosomal DNA from GAS and other streptococcal species was done as outlined by Kreikemeyer et al. (27). Plasmid DNA, transformation of *E. coli* and GAS, and other conventional manipulations were done essentially as described previously (49). Probes for Southern hybridization were generated by PCR, using digoxigenin-dUTP, as reported previously (47).

Construction of recombinant vectors and GAS strains. For the construction of the deletion mutant in serotype M49 strain 591, adjacent sequences of target genes on both sides were amplified from chromosomal DNA of strain 591 with the primers listed in Table S1 in the supplemental material. The resulting PCR products were cloned into MCS1 and MCS2 of pFW12 (48). This vector was designed for site-directed allelic replacement experiments within operons, allowing mutagenesis without polar effects (48). The obtained plasmids were transformed into strain 591, and then transformants were selected on spectinomycin-containing agar plates. The deletion of target genes was confirmed by site-specific PCRs and Southern blot hybridization analyses.

To construct the complemented strains and *cpa* operon-overexpressing strain, the pAT18 vector was utilized to express target genes under the control of the *gyrA* promoter, which was amplified using primers P_{gyrF}/SacI (5′-GAGAGCTC ATCATGACAGTCTGAGTAG-3′) and P_{gyrR}/BamHI (5′-GCGGATCCCTCC TTTTCTAGTCAATACTA-3′).

For generation of the *prtF2* mutant, an internal fragment of the gene was amplified and cloned into pSF151 via BamHI and EcoRI sites. The resulting plasmid was integrated into the chromosome of strain 591. The correct integration at a single site was confirmed by site-specific PCR and Southern blot hybridizations.

Examples of the genetic nomenclature used for the mutants are as follows: Δ*srtA*, deletion mutant of the *srtA* gene; Δ*srtA* Δ*srtC2*, double deletion mutant; Δ*srtA*::*srtA*, complemented deletion mutant; Δ*srtA*::mock, mock-complemented version (transformed with empty complementation vector); and *prtF2* insertion mutant, insertional inactivation of the PrtF2-encoding gene.

For the construction of plasmids expressing recombinant surface proteins from strain 591, the truncated genes without regions encoding the signal sequence and sorting signal were amplified using primers listed in Table S1 in the supplemental material. The fragments were cloned into pQE30 and transformed into *E. coli* XL10-Gold.

Immunogold labeling and transmission electron microscopy. The GAS WT and its isogenic mutants were grown overnight in THY medium, washed, and resuspended in phosphate-buffered saline (PBS). The bacterial suspension was added to Formvar-coated nickel grids and allowed to settle for 5 min. The bacteria on the grids were fixed with 1% paraformaldehyde-PBS for 5 min at room temperature and incubated with blocking buffer (2% bovine serum albumin [BSA], 5% skim milk containing blocking reagent, PBS) for 30 min. The grids were then exposed to polyclonal mouse or rabbit antisera (1:100 in blocking buffer) for 30 min and washed five times with PBS, followed by incubation with secondary gold-conjugated antibodies (5 nm or 10 nm) diluted 1:50 in blocking buffer. After being washed with PBS and then distilled water, the grids were air dried and examined in a Libra 120 transmission electron microscope (Carl Zeiss).

Immunofluorescence labeling of M protein and FctA. GAS cells were grown to exponential phase and fixed with 1% paraformaldehyde for 5 min at room temperature. After being washed two times with PBS, the cells were blocked with blocking buffer containing 2% BSA, 5% skim milk, and 5% fetal calf serum for 1 h at room temperature, followed by immunolabeling with anti-M protein or anti-FctA mouse antiserum (diluted 100 times with PBS–10% blocking buffer) and anti-mouse immunoglobulin G (IgG)–Alexa fluor 594 (diluted 500 times with PBS–10% blocking buffer). Cells were then counterstained with SYBR green dye at a concentration of 1 μM for 10 min at room temperature and washed five times with PBS. Subsequently, cells were mounted on glass slides and inspected with a fluorescence microscope. Nonimmunized mouse serum was utilized for preparation of a negative control. Cells incubated with either nonimmunized mouse serum or nonimmunized rabbit serum showed no staining for all strains.

Extraction of cell wall fractions and preparation of immunoblots. GAS cells were grown overnight in THY medium and washed twice with PBS. The cells were suspended in 50 mM sodium acetate buffer containing 40% sucrose and 5 mM EDTA, 10 units of phage lysin C_1 (PlyC) was added as outlined by Köller et al. (25), and then the cells were incubated for 1 h at room temperature. The resulting protoplasts were sedimented by centrifugation at 14,000 × *g* for 10 min, and the supernatant was stored at −20°C.

Supernatant samples were separated in 3 to 10 or 5 to 20% precast gels (Invitrogen) and blotted onto polyvinylidene difluoride membranes. The membranes were blocked in ImmunoBlock (Dainippon Sumitomo Pharma), incubated for 1 h with either mouse or rabbit antiserum diluted 1:2,000 in PBS containing 0.2% Tween 20 (PBST), washed three times with PBST, and then incubated with horseradish peroxidase-conjugated second antibody (Bio-Rad) diluted 1:2,000 for 1 h. Following the washing steps, the membranes were developed with ECL Western blot reagents (Amersham).

Preparation of His-tagged recombinant protein and antisera. Hyperexpression of recombinant proteins was induced by adding 0.1 mM IPTG (isopropyl-β-D-thiogalactopyranoside) to mid-exponential-phase *E. coli* cells, and then growth was continued at 30°C for 5 h. Recombinant protein was purified with a QIAexpress protein purification system (Qiagen) as outlined in the manufacturer's instructions. Eluted protein was dialyzed against PBS and concentrated by ultrafiltration with a Centricon centrifugal concentrator (filters for 100-, 75-, 50-, 30-, 10-kDa-cutoffs were used [Amicon]). The amounts of recombinant proteins were determined using a bicinchoninic acid protein assay kit (Pierce).

Mouse antisera against Cpa, FctA, FctB, and protein F2 were raised by immunizing BALB/c mice with the purified recombinant proteins. Briefly, female BALB/c mice were vaccinated intradermally with a mixture of 100 μg of recombinant proteins in 50 μl of PBS and the same volume of complete Freund adjuvant, followed by two boosts with 50 μg of recombinant proteins with incomplete Freund adjuvant after 2 and 3 weeks. Whole blood was then collected after 4 weeks. Preparation of rabbit antiserum against Cpa was done as previously reported (31). Usage of antisera for immunofluorescence staining and microscopic inspection of labeled bacteria followed the protocols of Kreikemeyer et al. (32).

Mouse experiments. Five-milliliter overnight cultures of each strain were diluted into 75 ml of medium in the absence of antibiotics and then grown to a

Klett unit of 85. Cells were transferred to prechilled centrifuge bottles and vortexed for 10 min to break up streptococcal chains. The cells were centrifuged for 15 min at 8,000 rpm, resuspended in 5 ml of PBS, and vortexed for an additional 2 min. A 1:100 dilution of the cell suspension was used for cell counts, and a 2×10^9-CFU stock was prepared for each strain.

SKH1 hairless mice (Charles River) were injected with a mixture of 50 μl Cytodex beads (20 mg ml^{-1}) and 50 μl of the 2×10^9-CFU strain stock on the dorsal rear surface of the back, resulting in a final inoculation of 1×10^8 CFU/mouse. The remaining slurry was plated onto blood agar to assess viable counts. Mice were examined daily for lesion size.

Eukaryotic cell adherence and internalization. Human epithelial HEp-2 (ATCC CCL23) cells were maintained in Dulbecco's modified Eagle's medium (Gibco) supplemented with 10% fetal bovine serum (Gibco). Adherence to and internalization of HEp-2 cells were assessed by antibiotic protection assay (41). Briefly, HEp-2 cells were infected with GAS strains at a multiplicity of infection of 1:50 for 2 h. For quantification of bacterial adhesion, infected cells were washed with PBS and lysed with distilled water. Serial dilutions of the lysate were plated on THY agar plates to count CFU. For assessment of bacterial internalization, the cells were washed with PBS and incubated with Dulbecco's modified Eagle's medium supplemented with penicillin (50 units ml^{-1}) for an additional 2 h. The cells were then washed and lysed, and bacterial numbers were counted as described above.

Blood survival assay. Overnight cultures of the WT and mutant strains were inoculated into fresh medium and grown to exponential growth phase. Bacteria were harvested by centrifugation, set to an optical density at 600 nm of 0.25, and further diluted 1:10,000 in PBS. The CFU contained in this final suspension were determined by plating serial dilutions on blood agar plates. Bacterial numbers were found to be in the range of 5×10^3 to 10×10^3 CFU/ml for all assays. Twenty microliters of each suspension was incubated with 480 μl of heparinized blood for 3 h at 37°C with rotation. After this incubation, the remaining CFU were determined by plating and related to the initial inoculum, which was set to 100%.

Fluorescence-activated cell sorter (FACS) analysis. GAS strain 591 and its isogenic *cpa* operon deletion mutant were grown to mid-exponential phase in THY medium at various temperatures. The cells were washed twice in PBS, blocked with blocking buffer, and incubated with either anti-FctA mouse antiserum or anti-M protein antiserum (1:100 dilution; kindly provided by H. Courtney, Memphis, TN). Nonimmunized mouse sera were used as a control for nonspecific antibody binding. Cells were washed three times with PBS and incubated with fluorescein isothiocyanate-conjugated goat anti-mouse IgG or fluorescein isothiocyanate-conjugated goat anti-rabbit IgG (1:500 dilution) for 1 h at room temperature, followed by washing with PBS. The cells were resuspended in PBS and analyzed with a flow cytometer set at a collection rate of 50,000 events. The percentage of cells expressing either M protein or FctA was calculated with FlowJo software (Tree Star, Ashland, OR), using the data for cells labeled with nonimmune sera.

GAS adherence to matrix proteins and biofilm formation. For quantification of the binding of the WT and mutant strains to immobilized matrix proteins, 96-well enzyme-linked immunosorbent assay (ELISA) plates (Greiner Bio-One) were coated overnight at 4°C with 5 μg/well human matrix proteins (Sigma) in PBS. Plates were blocked with 1% BSA in PBS for 1 h at 37°C and washed in 0.05% Tween 20–PBS.

Early-stationary-phase GAS strains diluted to an optical density at 600 nm of 0.4 in PBS were incubated in the coated wells for 30 min at 37°C. As controls, GAS strains were incubated in noncoated and BSA-coated wells. After four washes with PBS, a goat anti-GAS–horseradish peroxidase conjugate (Dunn Labortechnik GmbH) diluted 1:5,000 in PBS was added, and the plates were further incubated for 1 h at room temperature. After four washes with PBS, bound antibodies were visualized using a TMB peroxidase enzyme immunoassay substrate kit (Bio-Rad). After 10 min, the reactions were stopped with 0.5% H_2SO_4, and the optical density at 450 nm was monitored.

Biofilm assays were performed as previously described (35, 40), with a minor modification. Briefly, overnight cultures grown in C medium (0.5% proteose peptone 3, 1.5% yeast extract, 10 mM K_2HPO_4, 0.4 mM $MgSO_4$, 17 mM NaCl, adjusted to pH 7.5) were diluted 10 times with the same medium and seeded in a 24-well plate. Duplicate plates were incubated at both 28°C and 37°C for 24 h and 48 h, respectively. After removal of medium, the plates were washed three times with PBS, and adherent bacteria were stained with 0.2% crystal violet for 10 min and washed two times with PBS. The stained bacteria were suspended in 100 μl of 1% sodium dodecyl sulfate, and then 70-μl aliquots were transferred to 96-well plates and the optical density at 540 nm was measured.

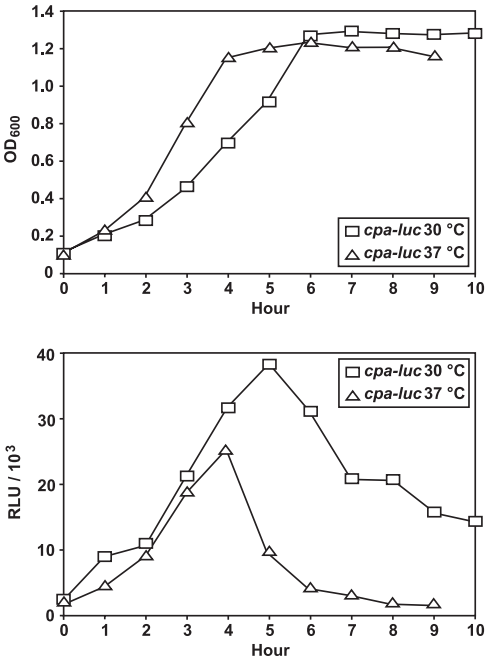

FIG. 2. Comparison of temporal luciferase activities from *cpa-luc* grown at different incubation temperatures. The strains were grown in THY medium under a CO_2-enriched atmosphere. Luciferase activities and culture densities were measured at 30°C and 37°C at hourly intervals. Data for one representative experiment of three independent experiments are shown. OD_{600}, optical density at 600 nm; RLU, relative light units.

Quantitative assays for luciferase activity. Construction of the *cpa-luc* strain has been reported previously (31), and the measurements were performed essentially as described previously (43).

Statistical analysis. Statistical analysis was performed with the Mann-Whitney U test or one-way analysis of variance and Scheffe's test. A confidence interval with a P value of <0.05 was considered significant. The infection model data were evaluated by an unpaired t test (two-tailed).

RESULTS

Pilus expression in a serotype M49 GAS strain. It has been reported that surface proteins encoded by the five-gene *cpa* operon form pilus-like appendages (42). To gain insight into pilus expression on the surface of the serotype M49 strain 591, we constructed an appropriate panel of *cpa* operon replacement mutants, i.e., deletions of the complete *cpa* operon and, additionally, the single *cpa*, *fctA*, *fctB*, *srtC2*, and *lepA* genes (Fig. 1). For all single-gene deletion mutants, the respective in *trans* complementation strains were also constructed and investigated. A novel *prtF2* insertion mutant was constructed as outlined in Materials and Methods.

As a first set of experiments, we assessed the growth conditions for peak expression of the *cpa* operon. Employing a *cpa-luc* reporter fusion strain (31), the *cpa* operon transcription rate was twice as high at 30°C as that at 37°C (Fig. 2). This difference is even more significant considering the decreased specific growth rate and increased generation time observed at an incubation temperature of 30°C (Fig. 2).

In order to prove if this temperature-sensitive transcription also leads to higher protein expression levels, we investigated

the localization and expression of FctA on the GAS surface under different temperatures, employing immunofluorescence microscopy and FACS analyses. The fluorescence microscopy pictures in Fig. 3A support three major observations. First, an increased fraction of GAS cells expressed FctA at a lower growth temperature. Second, at any growth temperature, only a subpopulation of cells expressed FctA, and third, FctA expression was apparently more abundant at the old poles of the cells. Several control experiments indicated the specificity of this observation (Fig. 3B and C), as follows: (i) expression of the M protein was independent of the growth temperature, (ii) this protein was expressed in a temperature-independent manner by the complete population, and (iii) deposition of the M protein was found to be circumferential and not restricted to the old poles (Fig. 3B).

As an approach to quantify these observations, FACS analysis was conducted (Fig. 3D). From the obtained data (Fig. 3D), we could calculate that 20% of the investigated GAS M49 population expressed FctA at 37°C. The percentage of FctA-positive cells increased to 47% if bacteria were incubated at 30°C. Two different peaks, which were more pronounced at 30°C, could be distinguished from FctA-stained and unstained cells. The percentage of M protein-expressing cells remained almost constant under the temperatures investigated, and just one peak was observed at both incubation temperatures. Together, these data support the observations for immunofluorescently stained GAS cells. They also suggest a bistable expression mode for FctA, which consequently might correlate with complete pilus expression. For optimum expression rates, the bacteria were thus grown at the lower temperature in subsequent experiments aiming at pilus detection.

FctA surface expression and pilus incorporation. As a second set of experiments, we aimed to detect surface-localized FctA in immunoblot experiments. The cell wall fraction of the WT and mutant strains was extracted with PlyC treatment (25). Expressed FctA in the protein extracts was detected using a mouse polyclonal antiserum against recombinant FctA (Fig. 4).

Detection and development of this blot revealed typical ladders of high-molecular-mass bands in the lanes containing surface proteins of the M49 WT strain (Fig. 4). The ladder pattern is due to various numbers of FctA molecules in pili from different GAS cells and has previously been reported for other GAS serotypes (42).

FctA expression and detection in the ladder bands were affected by Cpa and FctB deletions (Fig. 4, lanes 3 and 9, respectively) and were found to be abolished in the SrtC2, SrtA, and LepA deletion mutants (Fig. 4, lanes 7, 12, and 16, respectively). Moreover, the roughly 35-kDa monomeric form of FctA could not be found in the surface extracts of the FctB, SrtC2, and SrtA mutant strains (Fig. 4, lanes 9, 7, and 12, respectively). In contrast, deletion of Cpa and the putative signal peptidase LepA still allowed for appearance of the FctA protein in its monomeric form on the surfaces of the bacteria (Fig. 4, lanes 3 and 16, respectively). Consistently, no FctA protein was detected in the Cpa operon and FctA deletion mutants (Fig. 4, lanes 2 and 5, respectively).

Notably, some expression levels of the complemented mutant strains did not completely reach WT levels. This was most probably due to a constitutive and thus untimely expression of

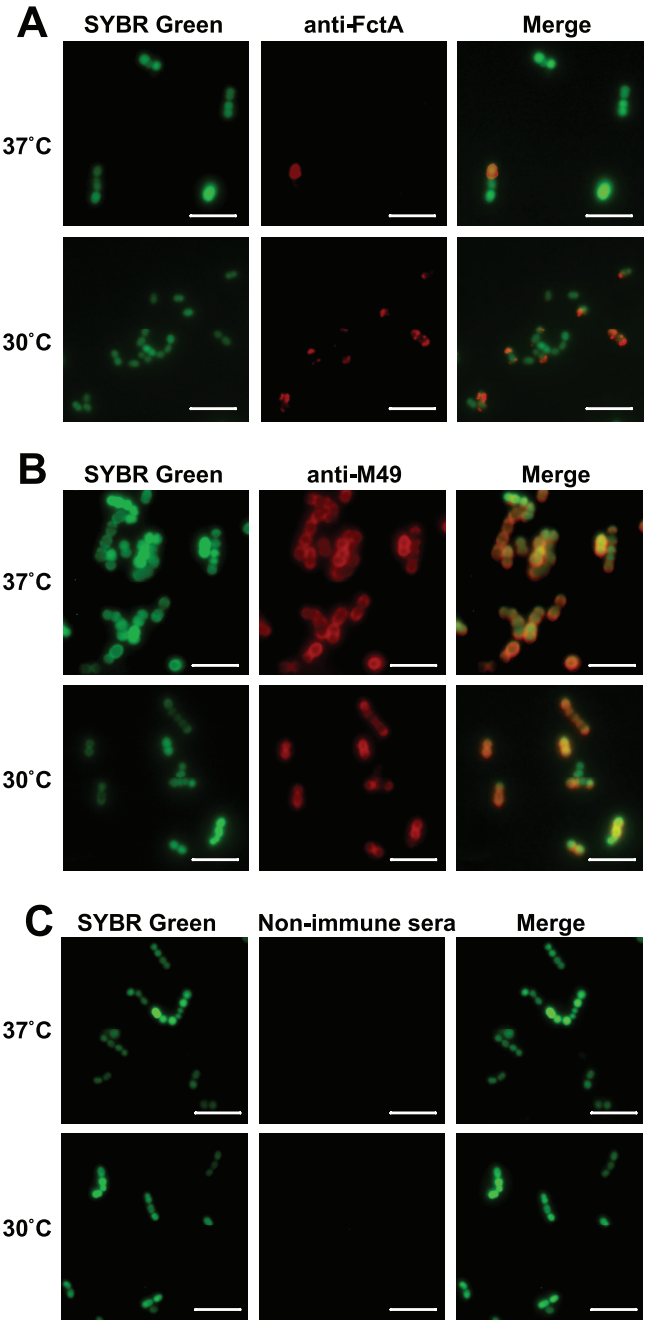

FIG. 3. Localization and expression of FctA and M protein on the GAS surface at different temperatures. (A to C) GAS cells grown at either 30°C or 37°C were immunolabeled with anti-FctA antiserum (A), anti-Emm antiserum (B), and nonimmunized mouse serum (C), followed by staining with Alexa fluor 594-labeled secondary antibody. Subsequently, the cells were counterstained with SYBR green. Bars, 5 μm. (D) Flow cytometric analysis of surface display of FctA (upper left and lower left panels) and M protein (upper right and lower right panels). For the detection of FctA, the WT (dark gray; left panels) and the *cpa* operon deletion mutant strain (light gray; left panels), grown to mid-exponential phase at 37°C (upper panels) and 30°C (lower panels), were labeled with anti-FctA serum and analyzed by FACS. As a negative control, nonimmune mouse serum was used (data not shown). As for the detection of M protein, the WT strain grown under the same conditions was labeled with anti-Emm antiserum (dark gray; right panels). Nonimmunized rabbit serum was used as a control for nonspecific antibody binding (light gray; right panels). Representative data from three experiments are shown.

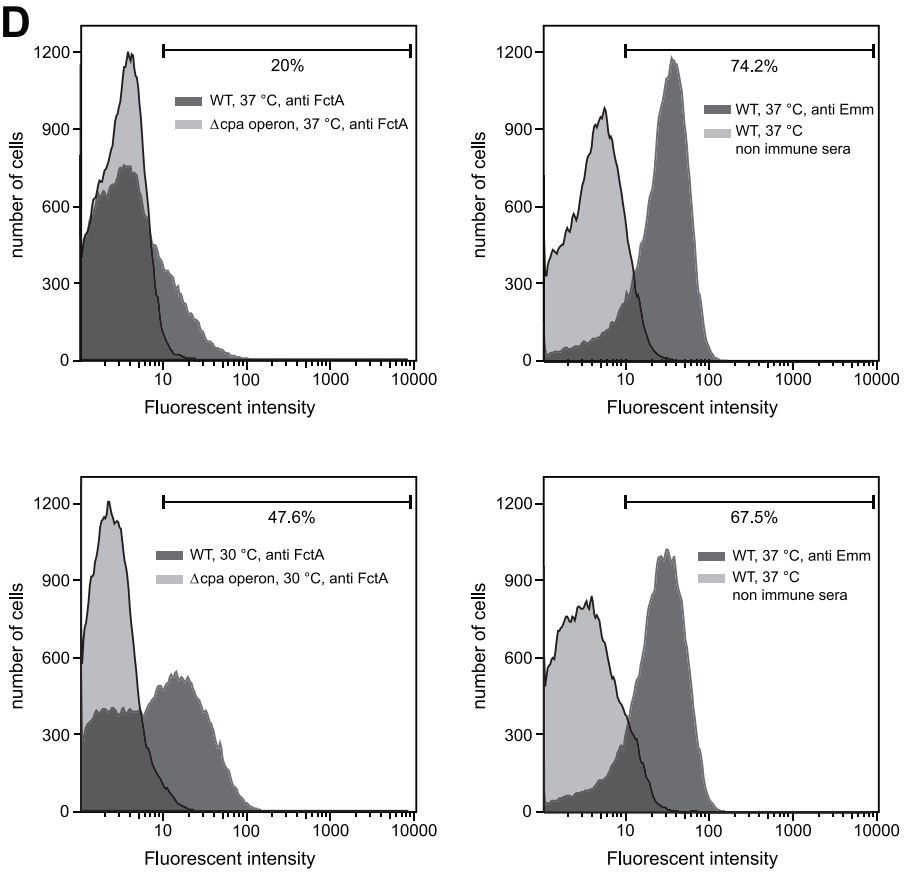

FIG. 3—*Continued.*

the complementation constructs. Complementation of LepA was obviously not affected in such a way (Fig. 4, lanes 16 and 17), whereas FctA complementation led to higher-than-WT-level expression amounts, as indicated by large amounts of the corresponding monomeric form (Fig. 4, lane 6).

Colocalization of Cpa in the FctA pilus shaft. Based on transmission electron micrographs, several of our attempts failed to document extended pilus structures on the surfaces of WT M49 bacteria under optimum conditions (30°C) (data not shown), although the results shown in Fig. 3 illustrate that at least FctA is surface expressed.

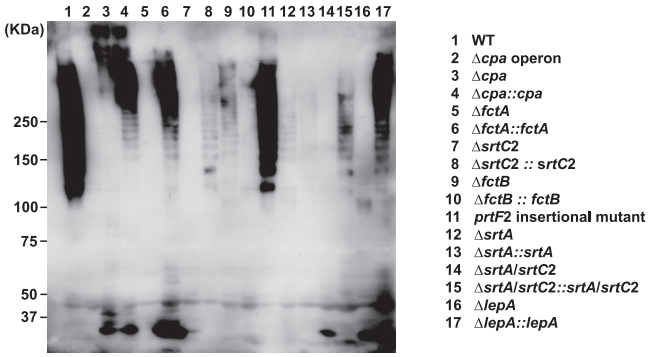

FIG. 4. Detection of pilus-like structures by immunoblotting. An immunoblot of the cell wall fraction of GAS strains after reaction with antiserum against FctA is shown.

In order to unequivocally demonstrate the expression, assembly, and presence of the pilus on the surface of the M49 serotype GAS strain, we constructed a recombinant strain which overexpressed the entire *cpa* operon in *trans* from a shuttle plasmid under the control of the constitutive *gyrA* promoter in the WT background and investigated whether increased amounts of pilus components and responsible enzymes, including sortase and the putative signal peptidase, induce the production of more abundant pilus structures than those in the WT strain. Immunogold staining of FctA on cells in transition from the log to the stationary phase of growth then allowed the discovery of pilus structures with approximate lengths of 1 to 2 μm (Fig. 5A and B). However, even in this *cpa* operon overexpression strain, long pilus structures could only occasionally be observed by transmission electron microscopic analysis. Utilizing this strain and a double-labeling method, the Cpa antigen was detected in close proximity to the FctA antigen (Fig. 5B). Notably, Cpa was observed at the pilus base, while the pilus backbone was composed exclusively of the FctA antigen.

Identification and detection of the T-antigen structure in a serotype M49 strain by use of anti-T14 monovalent serum. Although it was previously reported that FctA is the main backbone protein in a pattern D FCT-3-type M53 strain (42),

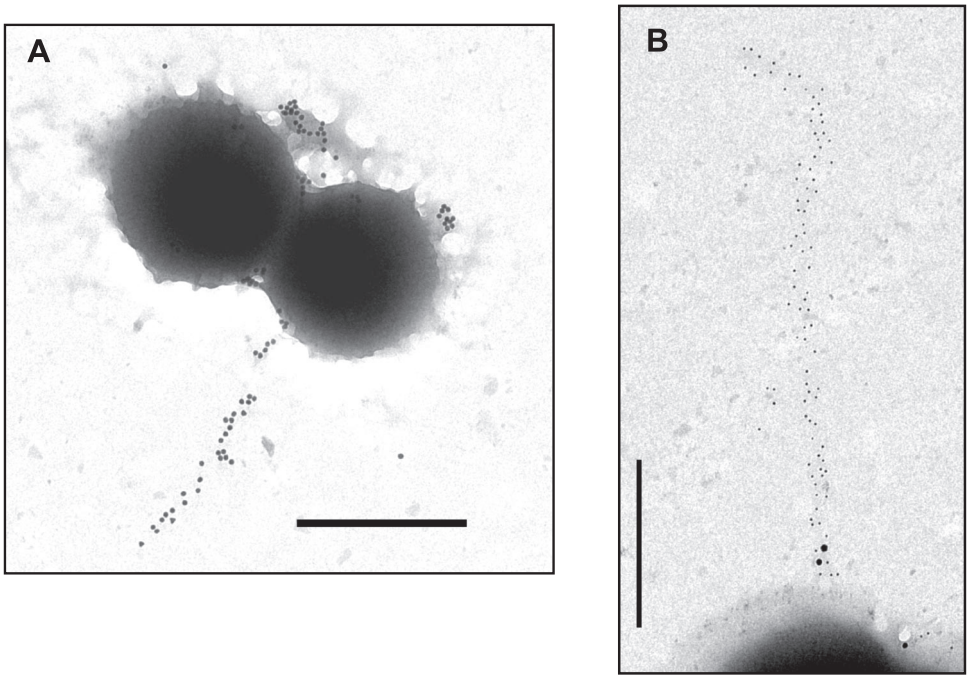

FIG. 5. Immunogold staining of FctA and Cpa in the *cpa* operon-overexpressing GAS strain. (A) Immunogold labeling of FctA in the M49 GAS strain with *cpa* operon overexpression. Bar, 1.0 μm. (B) Colocalization of FctA and Cpa. FctA and Cpa were immunolabeled with 10- and 20-nm-diameter gold particles, respectively. Bar, 0.5 μm.

the emerging scheme of serotype-specific surface protein features among GAS strains (36, 37) led us to study the nature of the T antigen in M49 GAS. The monovalent anti-T14 antiserum has been reported to be useful for identification of serotype M49 GAS strains (23). Thus, a variety of 11 recombinant proteins from a serotype M49 strain and 3 proteins from a serotype M6 strain were cloned, expressed as His-tagged fusion proteins in *E. coli*, overexpressed, purified, and subjected to sodium dodecyl sulfate-polyacrylamide gel electrophoresis, with subsequent blotting and immunoblot detection employing T6 and T14/T49 typing sera (see Fig. S1 in the supplemental material). Serving as a positive control and confirming earlier observations (20, 42), the anti-T6 monovalent serum exclusively detected the intense bands of recombinant T6 and FctX proteins from GAS serotype M6.

In contrast, the monovalent T14 typing serum reacted strongly with the recombinant serotype M49 FctA protein, with minor reactivity against the recombinant serotype M49 Cpa protein. These results clearly identified the GAS serotype M49 FctA protein as the major T antigen of this serotype. Based on the present data, the participation of Cpa in a complex together with FctA, comprising the T antigen of M49, cannot formally be excluded.

Requirement of sortase activity for GAS adherence, internalization, phagocytosis resistance, and biofilm formation. In order to characterize the distinctive functional and virulence-associated roles of the housekeeping sortase (SrtA) and the accessory sortase (SrtC2) encoded in the FCT-3 region of the M49 serotype GAS strain (Fig. 1), the individual sortase deletion mutants and the double sortase deletion mutant in the genetic background of GAS serotype M49 strain 591 were used in several pathogenesis-related assays. Moreover, to exclude the possibility that the phenotypes of the mutants were due to compensatory mutations on the chromosome, all specific mutant strains were complemented in *trans* with either a recombinant plasmid carrying the respective *srt* gene under the control of the constitutive *gyrA* promoter or an empty plasmid used as a negative control to exclude effects from the vector alone.

As a first approach to judge the impact of both sortases, the binding of the WT and mutant strains to immobilized extracellular matrix proteins was studied by ELISA (Fig. 6). In contrast to the robust binding of the WT strain to fibronectin (Fig. 6A) and fibrinogen (Fig. 6B), the *srtA* mutant, the double sortase mutant, and the mock-complemented strains showed significantly attenuated affinities for both matrix proteins. The binding was completely recovered in the respective complemented strains, suggesting an exclusive dependence of fibronectin and fibrinogen binding on the surface-anchoring activity of SrtA. Mutation of *srtC2* alone had no effect on fibronectin and fibrinogen binding. Binding to laminin (Fig. 6C) and collagen type IV (Fig. 6E) was also apparently dependent on SrtA and was not affected by the deletion of *srtC*2.

In contrast, binding of GAS strains to human collagen type I (Fig. 6D), mediated mainly by Cpa in a serotype M49 strain (31), was found to be reduced in both the *srtA* and *srtC2* single-gene mutants. This observation was further supported by the values measured for the double sortase mutant, which were lower than those for the two single-gene mutants. The binding of all complemented strains to collagen type I was completely or partially restored. These results indicate that SrtA is a prerequisite for the surface display of GAS proteins responsible for binding to fibronectin, fibrinogen, laminin, and collagen type IV. In contrast, the binding of *cpa* gene-carrying

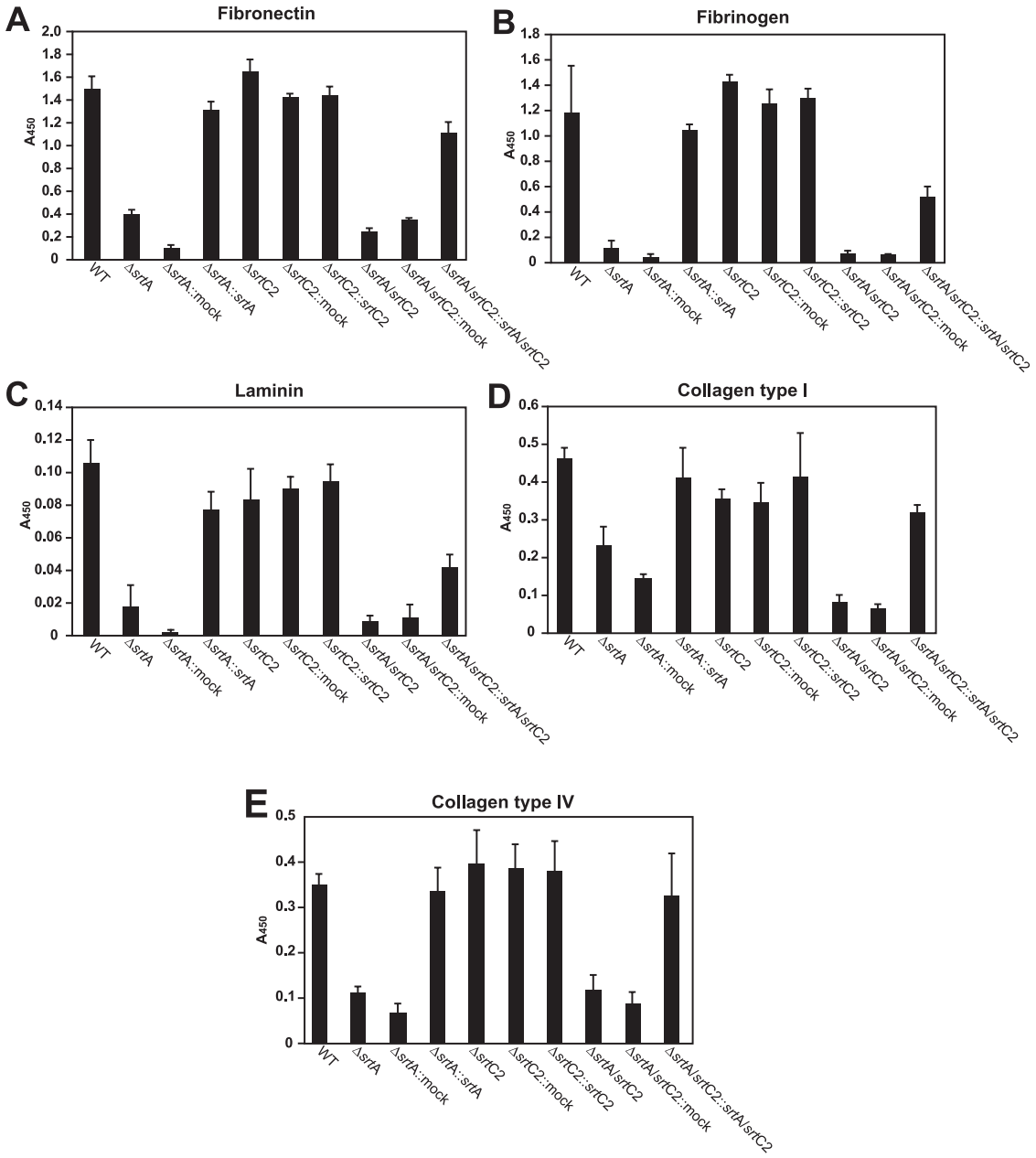

FIG. 6. Binding of the WT and mutant strains to immobilized human matrix proteins. Microtiter plates were coated with the indicated matrix proteins (fibronectin [A], fibrinogen [B], laminin [C], collagen I [D], and collagen IV [E]) and subsequently incubated with the GAS strains. Binding was detected by anti-GAS polyclonal antibody and is represented by the A_{450}. The data represent the mean values ± standard deviations for three independent experiments.

GAS to collagen type I obviously relies on the functions of both SrtA and SrtC2.

Next, we tested whether the altered mode of the *srt* mutants for binding of the extracellular matrix proteins subsequently affected their eukaryotic cell adhesion and internalization capabilities (Fig. 7). Consistent with the binding capacities observed in ELISAs, both adherence and internalization rates were reduced in the *srtA* and double sortase mutants and were restored in the complemented strains compared to WT levels (Fig. 7). In contrast, the *srtC*2 mutant showed no significant changes in adherence to and internalization into host cells.

We then determined the ability of the WT and sortase mutants to survive incubation in whole human blood (Fig. 8). Again, exclusively the *srtA* and double sortase mutants were attenuated in their efficiency at multiplying in whole human blood. This effect was at least partially restored in the corresponding complemented strains. This suggests that an important virulence factor for blood survival, most probably the M49 M protein (47), is linked to the GAS surface via SrtA. Mutation of the gene encoding SrtC2 did not impair the ability of the bacteria to multiply in blood. These results clearly indicate that SrtA contributes exclusively to one avenue of immune

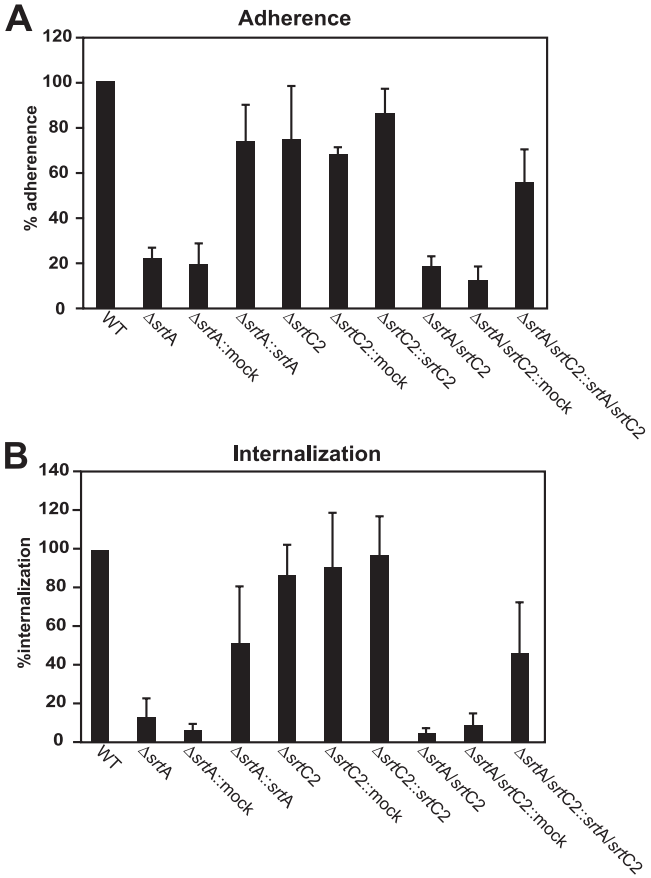

FIG. 7. Adhesion to (A) and internalization into (B) human epithelial cells. HEp-2 cells were infected with the indicated GAS strains at a multiplicity of infection of 1:50. The adherence and internalization were measured and calculated as described in Materials and Methods. The data represent the mean values ± standard deviations for three independent experiments. The value for the WT strain was set to 100% for each independent test.

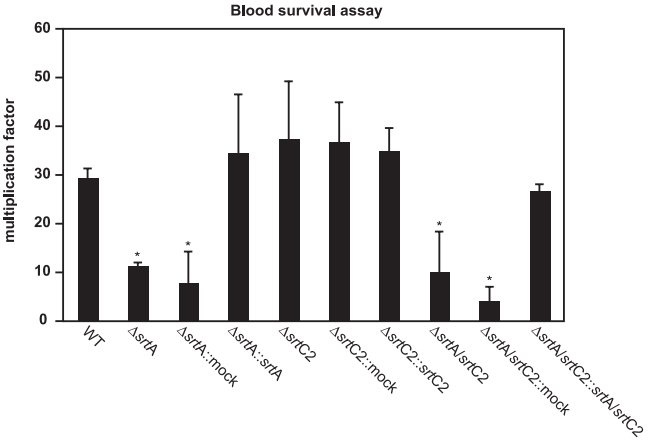

FIG. 8. Survival of WT and sortase mutant strains in human whole blood. The blood survival assay was conducted with GAS strains and heparinized human whole blood. The number of surviving CFU was determined by plating serial dilutions and subsequent colony counting. The *y* axis shows the resulting multiplication factor for each strain calculated from the percentage of surviving CFU related to the inoculum CFU. Due to the high variability of this assay depending on the blood donor, only data for one representative experiment are shown. However, in three independent experiments with blood from different donors, the same general survival tendencies were noted. *, significantly different from WT levels ($P < 0.05$).

evasion, which in turn could be critical for the establishment of GAS infections.

Lembke et al. recently reported that GAS strains are able to form biofilms under static and flow conditions (35), and a study by Manetti et al. found pilus expression to be associated with biofilm phenotypes (40). Thus, we next tested the ability of all mutants to form biofilms, using C medium as the growth medium. With that culture medium, even cells of the previously non-biofilm-building serotype M49 (35) form biofilms of significant mass. As shown in Fig. 9A and B, the SrtA mutant demonstrated significantly smaller amounts of biofilm, irrespective of the temperature used. That finding suggested that neither SrtC2 nor any other *cpa* operon-encoded protein plays a role in biofilm formation of the serotype M49 GAS strain.

Importance of sortase activity for GAS model skin infections. To test whether SrtA and/or SrtC2 of the GAS M49 serotype FCT-3 strain contributes to the development of skin infections, a mouse skin infection model was utilized to test the capability of the WT and its isogenic mutants to cause superficial skin lesions.

The mice infected with the WT strain developed purulent skin lesions, which were first observed at 3 days postinfection (Fig. 10). The lesion size gradually increased until 5 days postinfection. Surprisingly, and in contrast to the results of the in vitro matrix protein binding assay, the host cell adherence/internalization assays, and the blood survival assays, both sortase mutants caused larger purulent lesions than those in mice infected with the WT strain. Yet only the changes achieved with the SrtC2 mutant reached the level of significance. Mice infected with the double sortase knockout strain showed the largest and most severe skin lesions, again clearly above the level of significance (Fig. 10). This unexpected phenotype was completely or partially reverted by complementation with the sortase genes. Overall, functional impairment of mainly the M49 SrtC2 activity had a dramatic effect and led to an amplification of virulence in this particular animal model.

DISCUSSION

One of the initial steps of infection in GAS pathogenesis is the firm attachment of bacteria to host surfaces. Although a large number of GAS adhesins mediating these processes have been characterized in recent years (12, 13, 28), the molecular background of GAS tissue site preference was still elusive. Now it becomes evident that proteins encoded in a discrete genomic region of the GAS chromosome, called the FCT region, could be responsible to a major extent for GAS tissue tropism (26, 36, 46). Coincidently, at least some of the FCT region-encoded proteins are required for pilus formation in GAS (42, 55). However, neither the general biological role of GAS pili, if any, nor the function of many of the FCT region genes is currently well defined among different GAS serotype strains. Thus, the major task of this study was the molecular and functional characterization of so far scarcely defined genes/proteins and examination of their biological significance

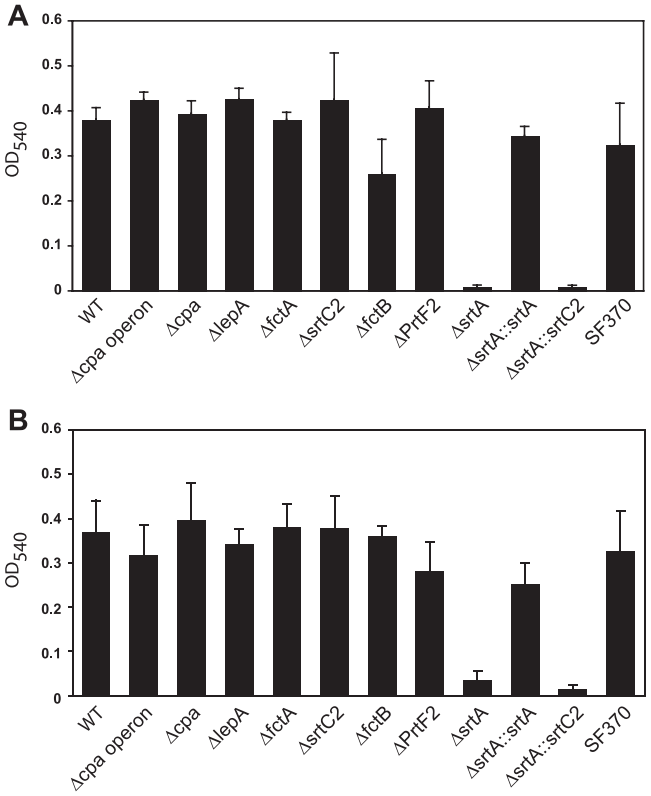

FIG. 9. Biofilm formation of GAS M49 WT strain and FCT mutants at different temperatures. The capacity of GAS strains to form biofilms on polystyrene plates was quantified by staining with crystal violet. The GAS strains were cultured at 37°C for 24 h (A) or at 28°C for 48 h (B) in C medium.

in pathogenesis assays and a mouse model of soft tissue infection. For this purpose, we based our investigation on the FCT-3 region in an M49 GAS serotype strain, which so far is the most abundant FCT type among all GAS serotypes tested (26, 46) but was still unaddressed in GAS pilus studies.

Based on the electron microscopy and immunoblot results presented here, we conclude with respect to pilus assembly that the *cpa* operon-encoded sortase (SrtC2) and signal peptidase I homologue (LepA) primarily act on the other *cpa* operon-encoded factors. Notably, SrtC2 mutation completely abolished FctA surface appearance, whereas LepA deletion still allowed monomeric FctA protein expression on the bacterial surface. An unexpected finding is that the housekeeping sortase (SrtA) also processes *cpa* operon factors.

On the other hand, the expression of LepA, the signal peptidase I homologue which was studied here for the first time in the FCT-3 M49 background, apparently is a prerequisite for the surface display of the pilus structure. Upon inspection of its deduced amino acid sequence, LepA is missing the conserved regions and critical residues for signal peptidase activity, i.e., the serine-lysine diad (45, 58), which in contrast is contained in the housekeeping signal peptidase I from GAS. This was strongly indicated by results from multiple alignment analyses with signal peptidases from both gram-positive and gram-negative bacteria. Exposing synthetic peptides encompassing the potential cleavage site or the full-length Cpa protein to recombinant LepA under conditions typically used for sortase digests and subjecting the molecules to high-performance liquid chromatography analysis did not reveal any LepA cleavage activity (data not shown). Based on these findings, it is likely that the GAS M49 LepA protein possesses no signal peptidase activity. This conclusion is supported by the observation of monomeric FctA surface expression/display in the LepA mutant. Restoration of LepA expression recovered the typical pilus ladder

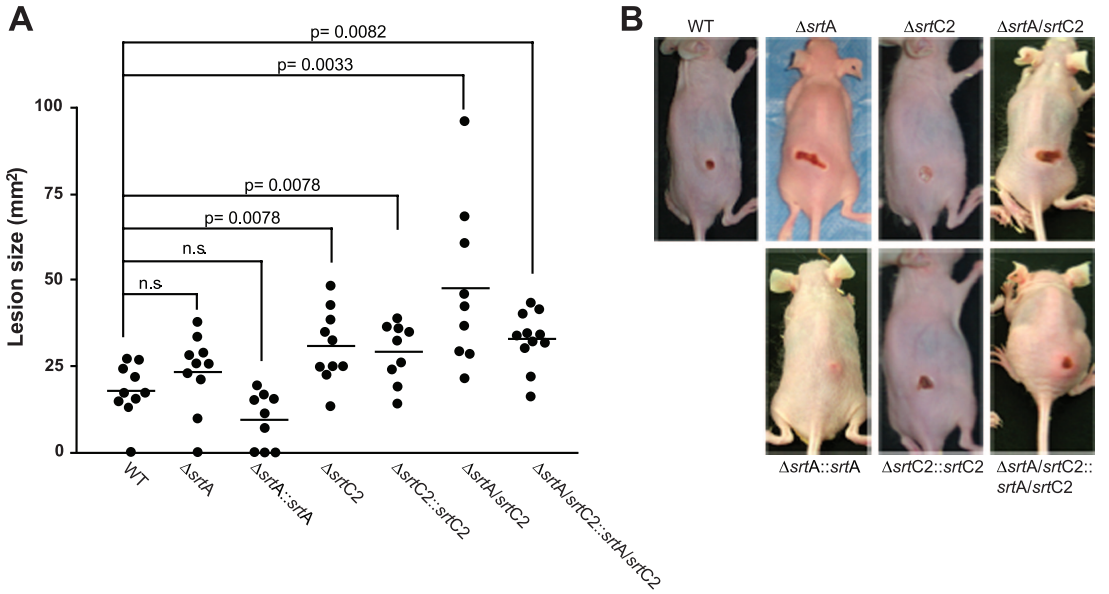

FIG. 10. Subcutaneous infection of SKH1 hairless mice with GAS M49 sortase mutants. (A) GAS strains (2×10^8 CFU) in a mixture with Cytodex beads were used to infect SKH1 mice. Lesion sizes were examined daily for up to 5 days postinfection. The graph shows data from the evaluation at 3 days postinfection. The bars represent average values, and significance values are indicated. n.s., no significant difference, as determined by Student's *t* test. (B) Representative pictures of mice were taken at 3 days postinfection.

band pattern. Thus, apparently, the unknown function of LepA is required for pilus assembly but not for monomeric FctA surface display. Therefore, we suspect that LepA is most likely a specialized enzyme for pilus components, acting with a crucial amino acid in its active center other than that reported for the housekeeping signal peptidases (45, 58). In contrast, the LepA equivalent SipA from a GAS M3 FCT-3 region was found to have chaperon-like activity if expressed in a heterologous M6 GAS strain (59). This observation further hints at serotype-specific functions of this class of enzymes among diverse GAS strains.

Comparing data on pilus assembly and function for GAS serotype strains and other species (36, 42, 55), many features are apparently at least species and most probably serotype dependent. A recent study has shown that FctA, Cpa, and protein F2 from a serotype T3/13/B3264 strain are involved in reactivity against the T-typing sera. Moreover, isogenic deletion mutants of *cpa*, *fctA*, and *prtF*2 were not T typeable (36). In the present study, the T14 typing serum (see Fig. S1 in the supplemental material) reacted with both Cpa (minor reactivity) and FctA (major reactivity) but not with FctB and protein F2. This suggests that the involvement of protein F2 with T-typing antiserum observed by Lizano et al. (36) was serotype specific. Moreover, protein F2 per se is not involved in pilus formation of the M49 serotype GAS strain, based on our immunoblot data.

FctA is also the major pilus backbone component in the serotype M49 strain. Cpa probably has stabilizing effects at the pilus base and is not included along the pilus shaft as an ancillary protein, as reported for other serotypes (42). Further support for the concept of serotype-specific activities among GAS proteins comes from a very recent study. In that study, the FCT-3 region RALP regulator Nra in an M53 GAS strain displayed an opposite polarity of its regulatory effects from that for the Nra regulator of the FCT-3 region of the M49 GAS strain (30, 37, 41, 49).

For another GAS serotype strain, it has been observed that pilus-like structures of GAS are preferentially expressed on cell poles (42). In cases where the surface display of Cpa on individual cells was examined by immunofluorescence or electron microscopy, its surface expression was found mainly at the old poles (31). These results are now confirmed and supported by our quantitative data (Fig. 3). More recently, Carlsson et al. (11) showed that the signal sequences of the M6 protein and protein F1 direct their secretion to different subcellular regions. The signal sequence of the M protein promotes secretion at the division septum, whereas that of protein F1 preferentially promotes secretion at the old pole. Based on these facts, it is likely that the signal sequences of pilus components, including Cpa, also determine the localized secretion on the cell surface. A common consensus signal sequence among Cpa, FctA, and FctB could not be identified in this study. Yet there is an FSIRK-like motif in the N-terminal portion of the full-sized Cpa protein. Although this motif was implicated in optimal secretion in *Staphylococcus aureus* (2), the YSIRK-like motif in the signal sequence of the M6 protein is apparently not required for its localized secretion (11). In a future study, the role of the signal sequence of pilus components as well as such a potential motif in Cpa on polarized secretion needs to be investigated.

Another potentially serotype-specific feature is the expression mode of the FctA pilus backbone protein in this FCT-3 and serotype M49 GAS strain, which strongly resembles a bistability phenotype (16). This conclusion is based on the fact that at 37°C, only 20% of all cells express FctA, while at 30°C, roughly 50% of a given population does so. Such a behavior has not been described for other GAS serotypes, although it is not clear whether those strains were investigated for this feature. The molecular background and biological benefit of the potential bistability phenomenon are currently unknown. Most likely, it could prepare a subpopulation of GAS cells for swiftly changing environmental conditions. However, bistability would preclude a general virulence function for pili encoded in this GAS FCT region or serotype.

When our serotype M49 strain was grown at 30°C, a temperature consistent with typical skin conditions, we noted an increased number of pilus structures. The other serotypes examined so far, including serotypes M1, M5, M6, and M12, apparently produced pilus appendages in higher abundance at 37°C (42). The responsible GAS regulators have not been defined for either the temperature dependence or the open circuit regulation-type expression of the *cpa* operon. So far, Nra and MsmR have been identified as the antagonistic regulators of the serotype M49 FCT-3 region genes (43). Other RALP-type regulators, such as RALP3 (30, 33) and RALP4/RivR (50), are encoded elsewhere on the GAS genome and were shown to superimpose FCT factor expression. Since these genes are present in various sequences and combinations in different serotype genomes, at least some serotype-dependent differences in pilus expression could be attributable to a specific constellation of the known regulators.

What is the biological function of pilus expression in GAS? For other streptococcal species, many virulence features have been attributed to pilus expression, including adherence to surfaces and endothelial cells (GBS) (15, 39), influence on cell interaction and inflammatory responses (pneumococci) (5), and biofilm formation and endocarditis (enterococci) (44). Most recently, Abbot and colleagues defined a role for GAS pili in adherence to keratinocytes (1). Moreover, Manetti and colleagues (40) have shown an involvement of the FCT-2 pilus region in GAS aggregation, microcolony formation, and biofilm phenotypes, suggesting a similar role of pili in the pathogenesis of all GAS strains (40). However, considering the functional data generated with factors from an FCT-3 region under the in vitro conditions of this study, the alternative FCT-3 region sortase (SrtC2) and pilus formation have no clearly defined roles in all in vitro pathogenesis assays performed. Neither binding of most kinds of matrix proteins, GAS adherence to and internalization into HEp-2 epithelial cells, survival in whole human blood, nor biofilm formation was significantly affected by pilus protein mutations. Still, pili could have a minor role in some of the assays. Because of the predominant activity of protein F2 in serotype M49 GAS for adherence to and internalization into HEp-2 cells (32), the effect of mutation in the pilus genes could hardly be detectable in the WT background. Consequently, an investigation of pilus assembly, expression, and function in a heterologous system could shed light on this issue. Among these functional assays, only binding to collagen I could to some extent be attributed specifically to

SrtC2 and pilus protein functions. Whether this feature contributes to tissue specificity of GAS strains is currently unclear.

Moreover, the observation of bistable expression modes proposes a reevaluation of data published on functional aspects of pili in GAS pathogenesis/virulence. If bistability of pilus expression in GAS is a serotype-independent phenotype, then the currently available data from published studies do not address the question of whether the data just represent an average of the population behavior, with one part expressing pili and another subpopulation not expressing pili.

In contrast to most of the above-mentioned functional assays, the results from the mouse skin infection model underscore an importance of the pilus factors for in vivo pathogenesis. Both the single SrtC2 mutant and the sortase double mutant revealed significant increases in virulence, as determined by the size and severity of ulcerative lesions in this particular animal model. Because of the attenuated host cell adherence and internalization, the sustained production of other surface and secreted virulence factors, such as proteases and capsule, could explain this behavior. Our observation is consistent with the hypothesis that an extracellular status renders GAS more aggressive at localized sites of skin infection in order to survive host defenses, whereas with an intracellular status the bacterium shuts down virulence factor expression in order to stay in a protected environment and not further attract the host immune system. This intra- or extracellular lifestyle may be correlated directly with either GAS persistence or purulent, severe, and cytotoxic disease manifestations (13).

In summary, we have shown that, to a large extent, the pilus protein composition and mode of assembly are GAS serotype dependent. Moreover, single pilus components were found almost exclusively at the old poles, and their expression mode resembled a bistability phenotype. Defining a clear role for pilus expression in GAS pathogenesis is a difficult task, at least under in vitro conditions, since obviously the effects of GAS pili are partly obscured by other non-FCT-3 region-encoded virulence factors. A much clearer picture emerged from the use of the GAS WT and isogenic sortase mutant strains in the mouse skin infection model. SrtC2 expression and, in consequence, pilus expression led to a less virulent phenotype in this infection model. This suggested a role for pilus expression in the delicate balance between eukaryotic cell adherence/internalization and cell destruction as well as tissue invasiveness. At least for the serotype M49 strain, our experiments indicated that pili do not act as virulence factors by definition but rather that expression of pili leads to an attenuated phenotype of GAS in the dermonecrosis model.

ACKNOWLEDGMENTS

We thank J. Normann, G. Fulda, R. Yasuda, and T. Matsumura for expert technical assistance. The pAT18 and pSF151 plasmids were kindly provided by P. Trieu-Cuot and L. Tao, respectively. We thank H. Courtney for generously providing anti-M protein serum. We also thank V. Fischetti and D. Nelson for providing PlyC.

This work was supported by a grant-in-aid for scientific research on priority areas from the Ministry of Education, Culture, Sports, and Technology (MEXT) (no. 18073011) and a grant-in-aid for scientific research (B) from the Japan Society for the Promotion of Science (no. 20390465) awarded to S.K. and by grants from the DFG (Po 391/12-1 and Kr1765/2-1) and BMBF grant BE031-03U213B, as a part of the German PathoGenomik Competence Network, awarded to A.P. and B.K. B.K. and A.P. further acknowledge support by BMBF grants 0313936A and 0313979B within the framework of the SysMo Systems Biology of Microorganisms and ERANet Pathogenomics competence networks, respectively.

REFERENCES

1. **Abbot, E. L., W. D. Smith, G. P. Siou, C. Chiriboga, R. J. Smith, J. A. Wilson, B. H. Hirst, and M. A. Kehoe.** 2007. Pili mediate specific adhesion of *Streptococcus pyogenes* to human tonsil and skin. Cell. Microbiol. **9:**1822–1833.
2. **Bae, T., and O. Schneewind.** 2003. The YSIRK-G/S motif of staphylococcal protein A and its role in efficiency of signal peptide processing. J. Bacteriol. **185:**2910–2919.
3. **Barnett, T. C., A. R. Patel, and J. R. Scott.** 2004. A novel sortase, SrtC2, from *Streptococcus pyogenes* anchors a surface protein containing a QVPTGV motif to the cell wall. J. Bacteriol. **186:**5865–5875.
4. **Barnett, T. C., and J. R. Scott.** 2002. Differential recognition of surface proteins in *Streptococcus pyogenes* by two sortase gene homologs. J. Bacteriol. **184:**2181–2191.
5. **Barocchi, M. A., J. Ries, X. Zogaj, C. Hemsley, B. Albiger, A. Kanth, S. Dahlberg, J. Fernebro, M. Moschioni, V. Masignani, K. Hultenby, A. R. Taddei, K. Beiter, F. Wartha, A. von Euler, A. Covacci, D. W. Holden, S. Normark, R. Rappuoli, and B. Henriques-Normark.** 2006. A pneumococcal pilus influences virulence and host inflammatory responses. Proc. Natl. Acad. Sci. USA **103:**2857–2862.
6. **Bessen, D. E., and A. Kalia.** 2002. Genomic localization of a T serotype locus to a recombinatorial zone encoding extracellular matrix-binding proteins in *Streptococcus pyogenes*. Infect. Immun. **70:**1159–1167.
7. **Beyer-Sehlmeyer, G., B. Kreikemeyer, A. Hoerster, and A. Podbielski.** 2005. Analysis of the growth phase-associated transcriptome of *Streptococcus pyogenes*. Int. J. Med. Microbiol. **295:**161–177.
8. **Bisno, A. L., F. A. Rubin, P. P. Cleary, and J. B. Dale.** 2005. Prospects for a group A streptococcal vaccine: rationale, feasibility, and obstacles—report of a National Institute of Allergy and Infectious Diseases workshop. Clin. Infect. Dis. **41:**1150–1156.
9. **Buccato, S., D. Maione, C. D. Rinaudo, G. Volpini, A. R. Taddei, R. Rosini, J. L. Telford, G. Grandi, and I. Margarit.** 2006. Use of *Lactococcus lactis* expressing pili from group B streptococcus as a broad-coverage vaccine against streptococcal disease. J. Infect. Dis. **194:**331–340.
10. **Carapetis, J. R., A. C. Steer, E. K. Mulholland, and M. Weber.** 2005. The global burden of group A streptococcal diseases. Lancet Infect. Dis. **5:**685–694.
11. **Carlsson, F., M. Stålhammar-Carlemalm, C. Flärdh, K. Sandin, E. Carlemalm, and G. Lindahl.** 2006. Signal sequence directs localized secretion of bacterial surface proteins. Nature **442:**943–946.
12. **Courtney, H. S., D. L. Hasty, and J. B. Dale.** 2002. Molecular mechanisms of adhesion, colonization, and invasion of group A streptococci. Ann. Med. **34:**77–87.
13. **Courtney, H. S., and A. Podbielski.** 2004. Group A streptococcal invasion of host cells, p. 239–274. *In* R. J. Lamont (ed.), Bacterial invasion of host cell. Cambridge University Press, Cambridge, United Kingdom.
14. **Cunningham, M. W.** 2000. Pathogenesis of group A streptococcal infections. Clin. Microbiol. Rev. **13:**470–511.
15. **Dramsi, S., E. Caliot, I. Bonne, S. Guadagnini, M. C. Prévost, M. Kojadinovic, L. Lalioui, C. Poyart, and P. Trieu-Cuot.** 2006. Assembly and role of pili in group B streptococci. Mol. Microbiol. **60:**1401–1413.
16. **Dubnau, D., and R. Losick.** 2006. Bistability in bacteria. Mol. Microbiol. **61:**564–572.
17. **Edwards, A. M., A. G. Manetti, F. Falugi, C. Zingaretti, S. Capo, S. Buccato, G. Bensi, J. L. Telford, I. Margarit, and G. Grandi.** 2008. Scavenger receptor gp340 aggregates group A streptococci by binding pili. Mol. Microbiol. **68:**1378–1394.
18. **Gianfaldoni, C., S. Censini, M. Hilleringmann, M. Moschioni, C. Facciotti, W. Pansegrau, V. Masignani, A. Covacci, R. Rappuoli, M. A. Barocchi, and P. Ruggiero.** 2007. *Streptococcus pneumoniae* pilus subunits protect mice against lethal challenge. Infect. Immun. **75:**1059–1062.
19. **Granok, A. B., D. Parsonage, R. P. Ross, and M. G. Caparon.** 2000. The RofA binding site in *Streptococcus pyogenes* is utilized in multiple transcriptional pathways. J. Bacteriol. **182:**1529–1540.
20. **Griffith, F.** 1934. The serological classification of *Streptococcus pyogenes*. J. Hyg. **34:**542–584.
21. **Hanski, E., and M. Caparon.** 1992. Protein F, a fibronectin-binding protein, is an adhesin of the group A streptococcus *Streptococcus pyogenes*. Proc. Natl. Acad. Sci. USA **89:**6172–6176.
22. **Hynes, W.** 2004. Virulence factors of the group A streptococci and genes that regulate their expression. Front. Biosci. **9:**3399–3433.
23. **Johnson, D. R., E. L. Kaplan, A. VanGheem, R. R. Facklam, and B. Beall.** 2006. Characterization of group A streptococci (*Streptococcus pyogenes*): correlation of M-protein and *emm*-gene type with T-protein agglutination pattern and serum opacity factor. J. Med. Microbiol. **55:**157–164.
24. **Kang, H. J., F. Coulibaly, F. Clow, T. Proft, and E. N. Baker.** 2007. Stabilizing isopeptide bonds revealed in gram-positive bacterial pilus structure. Science **318:**1625–1628.
25. **Köller, T., M. Nakata, D. Nelson, V. A. Fischetti, M. O. Glocker, A. Pod-**

bielski, and B. Kreikemeyer. 2008. Phagelysin C, a novel enzyme for compartment dependent proteomics of group A streptococci. Proteomics **8:**140–148.
26. **Kratovac, Z., A. Manoharan, F. Luo, S. Lizano, and D. E. Bessen.** 2007. Population genetics and linkage analysis of loci within the FCT region of *Streptococcus pyogenes*. J. Bacteriol. **189:**1299–1310.
27. **Kreikemeyer, B., M. D. Boyle, B. A. Buttaro, M. Heinemann, and A. Podbielski.** 2001. Group A streptococcal growth phase-associated virulence factor regulation by a novel operon (Fas) with homologies to two-component-type regulators requires a small RNA molecule. Mol. Microbiol. **39:**392–406.
28. **Kreikemeyer, B., M. Klenk, and A. Podbielski.** 2004. The intracellular status of *Streptococcus pyogenes*: role of extracellular matrix-binding proteins and their regulation. Int. J. Med. Microbiol. **294:**177–188.
29. **Kreikemeyer, B., K. S. McIver, and A. Podbielski.** 2003. Virulence factor regulation and regulatory networks in *Streptococcus pyogenes* and their impact on pathogen-host interactions. Trends Microbiol. **11:**224–232.
30. **Kreikemeyer, B., M. Nakata, T. Köller, H. Hildisch, V. Kourakos, K. Standar, S. Kawabata, M. O. Glocker, and A. Podbielski.** 2007. The *Streptococcus pyogenes* serotype M49 Nra-Ralp3 transcriptional regulatory network and its control on virulence factor expression from the novel ERES pathogenicity region. Infect. Immun. **75:**5698–5710.
31. **Kreikemeyer, B., M. Nakata, S. Oehmcke, C. Gschwendtner, J. Normann, and A. Podbielski.** 2005. *Streptococcus pyogenes* collagen type I-binding Cpa surface protein. Expression profile, binding characteristics, biological functions, and potential clinical impact. J. Biol. Chem. **280:**33228–33239.
32. **Kreikemeyer, B., S. Oehmcke, M. Nakata, R. Hoffrogge, and A. Podbielski.** 2004. *Streptococcus pyogenes* fibronectin-binding protein F2: expression profile, binding characteristics, and impact on eukaryotic cell interactions. J. Biol. Chem. **279:**15850–15859.
33. **Kwinn, L. A., A. Khosravi, R. K. Aziz, A. M. Timmer, K. S. Doran, M. Kotb, and V. Nizet.** 2007. Genetic characterization and virulence role of the RALP3/LSA locus upstream of the streptolysin S operon in invasive M1T1 group A streptococcus. J. Bacteriol. **189:**1322–1329.
34. **Lauer, P., C. D. Rinaudo, M. Soriani, I. Margarit, D. Maione, R. Rosini, A. R. Taddei, M. Mora, R. Rappuoli, G. Grandi, and J. L. Telford.** 2005. Genome analysis reveals pili in group B streptococcus. Science **309:**105.
35. **Lembke, C., A. Podbielski, C. Hidalgo-Grass, L. Jonas, E. Hanski, and B. Kreikemeyer.** 2006. Characterization of biofilm formation by clinically relevant serotypes of group A streptococci. Appl. Environ. Microbiol. **272:**2864–2875.
36. **Lizano, S., F. Luo, and D. E. Bessen.** 2007. Role of streptococcal T antigens in superficial skin infection. J. Bacteriol. **189:**1426–1434.
37. **Luo, F., S. Lizano, and D. E. Bessen.** 2008. Heterogeneity in the polarity of Nra regulatory effects on streptococcal pilus gene transcription and virulence. Infect. Immun. **76:**2490–2497.
38. **Maione, D., I. Margarit, C. D. Rinaudo, V. Masignani, M. Mora, M. Scarselli, H. Tettelin, C. Brettoni, E. T. Iacobini, R. Rosini, N. D'Agostino, L. Miorin, S. Buccato, M. Mariani, G. Galli, R. Nogarotto, D. V. Nardi, F. Vegni, C. Fraser, G. Mancuso, G. Teti, L. C. Madoff, L. C. Paoletti, R. Rappuoli, D. L. Kasper, J. L. Telford, and G. Grandi.** 2005. Identification of a universal group B streptococcus vaccine by multiple genome screen. Science **309:**148–150.
39. **Maisey, H. C., M. Hensler, V. Nizet, and K. S. Doran.** 2007. Group B streptococcal pilus proteins contribute to adherence to and invasion of brain microvascular endothelial cells. J. Bacteriol. **189:**1464–1467.
40. **Manetti, A. G., C. Zingaretti, F. Falugi, S. Capo, M. Bombaci, F. Bagnoli, G. Gambellini, G. Bensi, M. Mora, A. M. Edwards, J. M. Musser, E. A. Graviss, J. L. Telford, G. Grandi, and I. Margarit.** 2007. *Streptococcus pyogenes* pili promote pharyngeal cell adhesion and biofilm formation. Mol. Microbiol. **64:**968–983.
41. **Molinari, G., M. Rohde, S. R. Talay, G. S. Chhatwal, S. Beckert, and A. Podbielski.** 2001. The role played by the group A streptococcal negative regulator Nra on bacterial interactions with epithelial cells. Mol. Microbiol. **40:**99–114.
42. **Mora, M., G. Bensi, S. Capo, F. Falugi, C. Zingaretti, A. G. Manetti, T. Maggi, A. R. Taddei, G. Grandi, and J. L. Telford.** 2005. Group A streptococcus produce pilus-like structures containing protective antigens and Lancefield T antigens. Proc. Natl. Acad. Sci. USA **102:**15641–15646.
43. **Nakata, M., A. Podbielski, and B. Kreikemeyer.** 2005. MsmR, a specific positive regulator of the *Streptococcus pyogenes* FCT pathogenicity region and cytolysin-mediated translocation system genes. Mol. Microbiol. **57:**786–803.
44. **Nallapareddy, S. R., K. V. Singh, J. Sillanpää, D. A. Garsin, M. Höök, S. L. Erlandsen, and B. E. Murray.** 2006. Endocarditis and biofilm-associated pili of *Enterococcus faecalis*. J. Clin. Investig. **116:**2799–2807.
45. **Paetzel, M., A. Karla, N. C. Strynadka, and R. E. Dalbey.** 2002. Signal peptidases. Chem. Rev. **102:**4549–4580.
46. **Podbielski, A.** 2007. Flexible architecture of the *Streptococcus pyogenes* FCT genome region: finally the clue for understanding purulent skin diseases and long-term persistence? J. Bacteriol. **189:**1181–1184.
47. **Podbielski, A., A. Flosdorff, and J. Weber-Heynemann.** 1995. The group A streptococcal *virR49* gene controls expression of four structural *vir* regulon genes. Infect. Immun. **63:**9–20.
48. **Podbielski, A., B. Spellerberg, M. Woischnik, B. Pohl, and R. Lütticken.** 1996. Novel series of plasmid vectors for gene inactivation and expression analysis in group A streptococci (GAS). Gene **177:**137–147.
49. **Podbielski, A., M. Woischnik, B. A. Leonard, and K. H. Schmidt.** 1999. Characterization of *nra*, a global negative regulator gene in group A streptococci. Mol. Microbiol. **31:**1051–1064.
50. **Roberts, S. A., G. G. Churchward, and J. R. Scott.** 2007. Unraveling the regulatory network in *Streptococcus pyogenes*: the global response regulator CovR represses *rivR* directly. J. Bacteriol. **189:**1459–1463.
51. **Rosini, R., C. D. Rinaudo, M. Soriani, P. Lauer, M. Mora, D. Maione, A. Taddei, I. Santi, C. Ghezzo, C. Brettoni, S. Buccato, I. Margarit, G. Grandi, and J. L. Telford.** 2006. Identification of novel genomic islands coding for antigenic pilus-like structures in *Streptococcus agalactiae*. Mol. Microbiol. **61:**126–141.
52. **Scott, J. R., and D. Zähner.** 2006. Pili with strong attachments: gram-positive bacteria do it differently. Mol. Microbiol. **62:**320–330.
53. **Talay, S. R., P. Valentin-Weigand, P. G. Jerlstrom, K. N. Timmis, and G. S. Chhatwal.** 1992. Fibronectin-binding protein of *Streptococcus pyogenes*: sequence of the binding domain involved in adherence of streptococci to epithelial cells. Infect. Immun. **60:**3837–3844.
54. **Tao, L., D. J. LeBlanc, and J. J. Ferretti.** 1992. Novel streptococcal-integration shuttle vectors for gene cloning and inactivation. Gene **120:**105–110.
55. **Telford, J. L., M. A. Barocchi, I. Margarit, R. Rappuoli, and G. Grandi.** 2006. Pili in gram-positive pathogens. Nat. Rev. Microbiol. **4:**509–519.
56. **Terao, Y., S. Kawabata, M. Nakata, I. Nakagawa, and S. Hamada.** 2002. Molecular characterization of a novel fibronectin-binding protein of *Streptococcus pyogenes* strains isolated from toxic shock-like syndrome patients. J. Biol. Chem. **277:**47428–47435.
57. **Trieu-Cuot, P., C. Carlier, C. Poyart-Salmeron, and P. Courvalin.** 1991. Shuttle vectors containing a multiple cloning site and a *lacZ* alpha gene for conjugal transfer of DNA from *Escherichia coli* to gram-positive bacteria. Gene **102:**99–104.
58. **Tuteja, R.** 2005. Type I signal peptidase: an overview. Arch. Biochem. Biophys. **441:**107–111.
59. **Zähner, D., and J. R. Scott.** 2008. SipA is required for pilus formation in *Streptococcus pyogenes* serotype M3. J. Bacteriol. **190:**527–535.

Editor: V. J. DiRita